ISSN 1063-7834, Physics of the Solid State, 2020, Vol. 62, No. 9, pp. 1539–1542. © Pleiades Publishing, Ltd., 2020.
Russian Text © The Author(s), 2020, published in Fizika Tverdogo Tela, 2020, Vol. 62, No. 9, pp. 1375–1378.

SUPERCONDUCTIVITY

Superconducting Microstructures with High Impedance

K. V. Shein[a], A. A. Zarudneva[a], V. O. Emel'yanova[a], M. A. Logunova[a], V. I. Chichkov[b], A. S. Sobolev[c], V. V. Zav'yalov[a, d], J. S. Lehtinen[e, f], E. O. Smirnov[g], Yu. P. Korneeva[g], A. A. Korneev[g, a], and K. Yu. Arutyunov[a, d, *]

[a] *"Higher School of Economics" National Research University, Moscow, Russia*
[b] *National University of Science and Technology "MISIS", Moscow, Russia*
[c] *Kotel'nikov Institute of Radio Engineering and Electronics, Russian Academy of Sciences, Moscow, Russia*
[d] *Kapitza Institute for Physical Problems, Russian Academy of Sciences, Moscow, Russia*
[e] *VTT Technical Research Centre of Finland, Espoo, 02150 Finland*
[f] *Department of Physics, University of Jyvaskyla, PB 35, Jyvaskyla, FI-40014 Finland*
[g] *Moscow Pedagogical State University, Moscow, Russia*
**E-mail: karutyunov@hse.ru*

Received March 26, 2020; revised March 26, 2020; accepted April 2, 2020

Abstract—The transport properties of two types of quasi-one-dimensional superconducting microstructures were investigated at ultra-low temperatures: the narrow channels close-packed in the shape of meander, and the chains of tunneling contacts "superconductor-insulator-superconductor." Both types of the microstructures demonstrated high value of high-frequency impedance and-or the dynamic resistance. The study opens up potential for using of such structures as current stabilizing elements with zero dissipation.

Keywords: superconductivity, thin films, kinetic inductance, tunneling contacts, high impedance
DOI: 10.1134/S1063783420090280

1. INTRODUCTION

Deceleration in growth of level of integration of commercial micro- and nanoelectronic devices, formally signifying failure of the Moore's law [1], is evidenced in recent years. Two reasons can be given for this: large heat dissipation per unit volume (or per unit area) and various quantum-size effects. The comprehensive solution to the first problem can be the transition from the normal metals or semiconductors to superconducting materials, in critical elements of circuit. In line with this simplistic approach, use of superconducting RSFQ (rapid single flux quantum) logic makes it possible not only to significantly reduce the energy consumption but also to achieve the operation speed exceeding hundredfold the standard solutions based on CMOS (complementary metal-oxide semiconductor) technologies [2]. It is expected that the element base of quantum computers can also be constructed with use of superconducting materials.

One of the factors constraining the operation speed of superconducting nanoelectronic devices is their high kinetic inductance. However the effect of kinetic inductance can be useful in a number of applications. The interest in the physics of quasi-one-dimensional superconductors [3], in which fluctuations of the order parameter $\Delta = |\Delta|e^{i\phi}$ can be important, has been increased in recent years. More specifically, it was shown that specific manifestation of quantum fluctuations—quantum phase slip—is the process dual to Josephson tunneling [4–7]. The phase of the order parameter ϕ and quasicharge q are complex-conjugated values. Consequently, for high phase uncertainty (= strong fluctuations) it is necessary to fix the charge that, for electronic circuit, is equivalent to stabilization of the current which is the time derivative of the charge $I \equiv dq/dt$. The standard solution utilizing ballast resistors [8–10] is not free from shortcomings. More specifically, presence of high-resistance elements in the circuit inevitably results in presence of Johnson noise [11].

In this work, we studied operation of two types of microelectronic structures: thin superconducting channels with significant value of kinetic inductance and chains of superconductor-insulator-superconductor (SIS) tunnel contacts. Both systems demonstrate high impedance (at zero dissipation) on alternating current, and can be used as current stabilizing elements in various electronic circuits.

2. THEORY

The frequency and temperature dependencies of kinetic inductance L_k can be obtained using the standard models of superconductivity [12]. Within the

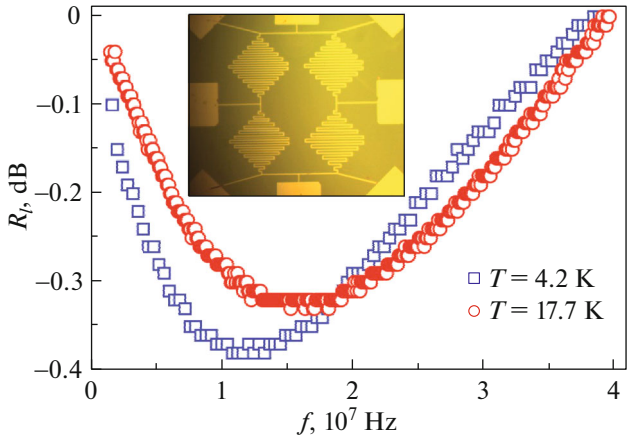

Fig. 1. Dependencies of magnitude of high frequency reflection coefficient R_l on frequency f for NbN microstructure with length $l = 50$ μm, thickness $d = 5$ nm, and line width $w = 100$ nm, packed to the area of 10×10 μm, at temperatures above and below the critical T_c(NbN) = 6.5 K. The inset demonstrates a microphotograph of the typical titanium structure: narrow superconducting strip close-packed in the shape of meander.

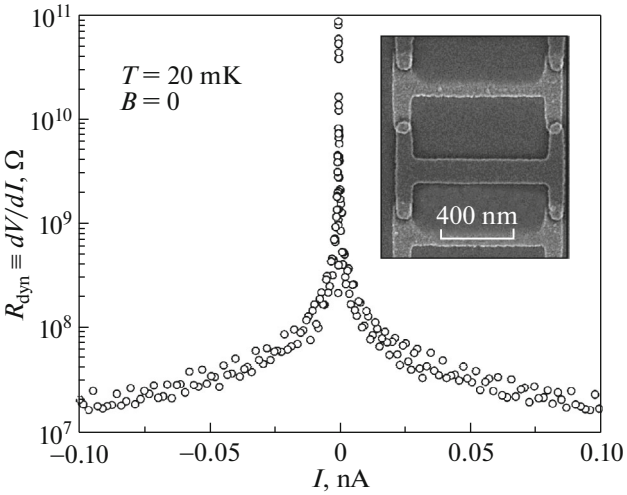

Fig. 2. Dependence of dynamic resistance $R_{dyn} \equiv dV/dI$ on bias current I for a chain of 25 pairs of tunnel contacts Al/AlO_x/Al|/.../AlO_x/Al (inset) in zero magnetic field and at ultra-low temperature $T = 20$ mK $\ll T_c$(Al) = 1.2 K.

Ginsburg–Landau equations, for the temperatures close to the critical temperature T_c, and at low bias current $I \to 0$ it is possible to obtain the following temperature dependence

$$L_k(T) = \frac{L_k(0)}{1-(T/T_c)}.$$

Bardeen–Cooper–Schrieffer microscopic model gives the simple expression for kinetic inductance of narrow superconducting channel

$$L_k = \frac{\hbar R_N}{\pi\Delta(T)} \frac{1}{\tanh\left\{\dfrac{\Delta(T)}{2k_BT}\right\}}.$$

Hence, superconducting materials with high resistance in normal state R_N and low critical temperature T_c can provide high values of kinetic inductance at low temperatures $T \ll T_c$. At ac current of not too high frequency $f < \Delta/h$, the impedance of such an element $Z_L(f) \sim fL$ can achieve considerable value, combined with zero dissipation in dc component [13, 14].

Use of tunnel SIS elements providing high dynamic resistance $R_{dyn} \equiv dV/dI \gg R_N$ at low currents, in other words, well below the quasi-particle region of the I–V dependence [15] can become alternative solution to high kinetic inductance. Dependence of the dynamic resistance on current $R_{dyn}(I)$ is highly nonlinear and tends to infinity at zero bias $I \to 0$.

3. SAMPLES AND EXPERIMENTAL TECHNIQUE

The microstructures constituting long and narrow channels close-packed in the shape of a meander (Fig. 1, inset) were manufactured by photolithography and vacuum metal deposition.

NbN and Ti by were chosen as materials for the superconducting structures. Thickness and width d/w of the films were equal to 5/100 nm and 30 nm/2 μm respectively. The resistivity per square in normal state was $R_{N\square}$(NbN) ≈ 950 Ω and $R_{N\square}$(Ti) = 200 Ω, respectively. The nanowires cross-sections were chosen predeterminedly larger than the dimensions where the contribution of thermal and/or quantum fluctuations is considerable for Ti [16–20] and NbN [21]. The dependencies of the resistance on temperature demonstrated the well defined superconducting transitions in the region T_c(NbN) = 6.5 ± 0.5 K and T_c(Ti) = 0.42 ± 0.02 K. Any nonmonotonicities of the shape of the $R(T)$ transition, which can be the signature of either inhomogeneity of the system [22], or its disequilibrium [23, 24], were not found.

The nanostructures constituting chains of identical components Al/AlO_x/Al/.../AlO_x/Al were manufactured by electron-beam lift-off lithography and multi-angle vacuum deposition (Fig. 2, inset) with critical temperature of superconducting aluminium T_c(Al) = 1.2 K.

All experiments were carried out at low and ultra-low temperatures. Measurements of the dependencies $R(T)$ and $V(I)$ were carried out with use of multi-stage system of the RLC-filters decreasing the influence of electromagnetic noise [25]. Measurements of current–voltage characteristics (I–V curves) and fre-

quency-response characteristics (FRC) was carried out by the standard 4-point contacts method.

4. RESULTS AND DISCUSSION

For measurement of I–V curves and FRC of quasi-one-dimensional superconducting channels, current in the circuit and voltage accross the sample were recorded simultaneously. The high frequency generator output was loaded by the 50 Ω cryogenic coaxial cable connected to the studied LC-circuit where L is unknown inductance of the microstructure, and C = 50 pF is the known capacity of the parallel-connected "ballast" capacitor. Preliminary measurements of the capacitor demonstrated that its capacity does not change much from room temperature to 2 K up to 400 MHz. In experiment, the reflection coefficient R_l was measured (in dB) as function of frequency of the probing signal

$$R_l = -20\log_{10}\left|\frac{Z_{\text{load}} - Z_{\text{source}}}{Z_{\text{load}} + Z_{\text{source}}}\right|,$$

where Z_{load} and Z_{source} are the load and source impedances, respectively. The dependencies $R_l(f)$ clearly demonstrate the minimum corresponding to the resonance frequency f_{res} of the system (Fig. 1). The shift of f_{res} to lower values while cooling of the system to superconducting state originates from the increase of impedance of the system. Considering the fact that the ballast capacity is constant, C = 50 pF, the magnitude of total inductance can be determined trivially: $L = L_k + L_m = (1/4\pi^2 C)(1/f_{\text{res}})^2$. In our case of the micron-scale superconducting system, the magnetic inductance L_m is substantially less than the kinetic inductance and is determined solely by geometry of the structure, and, therefore, is the same in normal and superconducting states. For the thin NbN film meander with the length l = 500 μm, thickness d = 5 nm, and the line width w = 100 nm, packed to the area 10 × 10 μm, using the dependencies $R_l(f)$ (Fig. 1), it is possible to estimate the inductance $L_k \approx 5$ μH at T = 4.2 K. The corresponding kinetic inductance per unit area in superconducting state $L_{k\square} \approx 0.75$ nH/□. Our results for the NbN structures are in a reasonable quantitative agreement with the literature data [12–14]. A little higher, in comparison with [12, 26], values of specific kinetic inductance can be explained by the increase of disorder in the studied NbN films that results in higher resistivity ($R_\square \approx 1$ kΩ in comparison with 875 Ω) and lower critical temperature (T_c = 6.5 K in comparison with 10 K). Variation of the bias current does not have an impact on the dependence $R_l(f)$. The high-frequency impedance achieves the value $Z_L(f) \approx 30$ kΩ on frequencies about 1 GHz that is not such an outstanding result. However manufacturing, by modern lithographic methods, of nanostructures with approximately hundredfold higher value of kinetic inductance without essential shunting by stray capacity is quite realistic. The appropriate high-frequency impedance of megaohm range already is quite sufficient for investigation of the quantum dynamics of charge within the wide ranges of frequencies and currents [9, 10, 27]. The qualitatively comparable results were obtained also on titanium microstructures (Fig. 1, inset). The particular aspects of the experiment in dilution refrigerator ^{3}He^{4}He at ultra-low temperatures T < 100 mK resulted in essentially larger measurement error $Z_L(f)$ for titanium. The effect probably occurs due to excessive heating of the tested structures by probing signal.

The transport properties of the chains Al/AlO$_x$/Al/.../AlO$_x$/Al (Fig. 2, inset) were studied at ultra-low temperatures $T \sim 20$ mK $\ll T_c$(Al) = 1.2 K. Parameters of oxidation of aluminium film were chosen so that the thickness of the tunnel barrier turned out to be large enough, and, as a consequence, the magnitude of the Josephson tunnel current turned out to be small: I_c < 10 pA. The related energy $E_J = \hbar I_c$ is much less than the charging energy $E_c = e^2/2C$ where C can be estimated as capacitance of series-connected plane capacitors with the dielectric layer of about ~2 nm in thickness, with the conductive plates area (contacts overlap) ~100 × 100 nm, and with dielectric constant of aluminum oxide ε ~ 10. The requirement $E_J \ll E_c$ results in dominating of charging effects over the Josephson's ones [28], and, accordingly, makes it possible to neglect the quantum fluctuations.

All structures Al/AlO$_x$/Al/...AlO$_x$/Al demonstrated the I–V curves typical for series-connected tunnel SIS-contacts. The dynamic resistance $R_{\text{dyn}} \equiv dV/dI$ obtained by numerical differentiation of the I–V curves, demonstrates the well defined singularity at small current bias approaching the value $R_{\text{dyn}}(I \to 0) \sim 10^{11}$ Ω (Fig. 2).

At high values of current, the dynamic resistance decreases, tending to the value $R_{\text{dyn}}(I \gg 0) \sim 10^5$ Ω corresponding to tunnel resistance of quasi-particle region of the I–V dependence. The latter observation limits utilization of SIS contacts as current stabilizing elements. Indeed, investigation of quantum dynamics of charge using chains of the SIS contacts made possible to register well defined Coulomb blockage, while at finite currents, the Bloch's singularities are strongly dithered even in comparison with the case of purely dissipative current electrodes made of high-resistive materials [27]. Seems that at finite currents, the superconducting current-biasing elements with high kinetic inductance should be preferred.

5. CONCLUSIONS

Transport properties of two types of quasi-one-dimensional superconducting microstructures were investigated: narrow channels with high magnitude of

kinetic inductance and the chains of tunnel SIS contacts. High magnitude of dynamic resistance of the SIS-contacts at low currents makes them highly effective for observation of such effects as the Coulomb blockade on the $I–V$ curves of quasi-one-dimensional superconducting channels governed by quantum fluctuations of order parameter [18]. However strong nonlinearity of the $I–V$ dependencies of the SIS contacts results in substantial drop of dynamic resistance at finite currents. On the contrary, narrow and long superconducting elements demonstrate high magnitudes of kinetic inductance which, in the region of finite, but not very high currents $I \ll I_c$, make it possible to obtain significant value of impedance on sufficiently high frequencies, providing the effective current stabilization.

FUNDING

Statement of the problem, analysis of the results, and drafting of the text of paper were carried out by K.Yu. Arutyunov and were supported by the project no. 19-01-050 under the HSE Academic Fund Program in 2019–2020, and under the state support by Russian Academic Excellence Project "5-100".

COMPLIANCE WITH ETHICAL STANDARDS

Conflict of interests. The authors declare that they have no conflicts of interest.

REFERENCES

1. G. Moore, Electronics **38**, 114 (1965).
2. K. K. Likharev and V. K. Semenov, IEEE Trans. Appl. Supercond. **1**, 3 (1991).
3. K. Yu. Arutyunov, D. Golubev, and A. D. Zaikin, Phys. Rep. **464**, 1 (2008).
4. A. D. Zaikin and S. V. Panyukov, Phys. Lett. A **120**, 306 (1987).
5. D. V. Averin and A. A. Odintsov, Phys. Lett. A **140**, 251 (1989).
6. A. D. Zaikin, J. Low Temp. Phys. **80**, 223 (1990).
7. J. E. Mooij and Y. V. Nazarov, Nat. Phys. **2**, 169 (2006).
8. L. S. Kuzmin and D. S. Havil, Phys. Rev. Lett. **67**, 2890 (1991).
9. T. T. Hongisto and A. B. Zorin, Phys. Rev. Lett. **108**, 097001 (2012).
10. J. S. Lehtinen, K. Zakharov, and K. Yu. Arutyunov, Phys. Rev. Lett. **109**, 187001 (2012).
11. C. H. Webster, J. C. Fenton, T. T. Hongisto, S. P. Giblin, A. B. Zorin, and P. A. Warburton, Phys. Rev. B **87**, 144510 (2013).
12. A. J. Annunziata, PhD Thesis (Yale Univ., New Haven, CT, 2010).
13. A. J. Kerman, E. A. Dauler, W. E. Keicher, J. K. W. Yang, K. K. Berggren, G. Gol'tsman, and B. M. Voronov, Appl. Phys. Lett. **88**, 111116 (2006).
14. A. J. Kerman, E. A. Dauler, J. K. W. Yang, K. M. Rosfjord, V. Anant, K. K. Berggren, G. Gol'tsman, and B. M. Voronov, Appl. Phys. Lett. **90**, 101110 (2007).
15. M. Tinkham, *Introduction to Superconductivity*, 2nd ed. (McGraw-Hill, New York, 1996).
16. J. S. Lehtinen, T. Sajavaara, K. Yu. Arutyunov, M. Yu. Presnjakov, and A. Vasiliev, Phys. Rev. B **85**, 094508 (2012).
17. K. Yu. Arutyunov, J. S. Lehtinen, and T. J. Rantala, J. Supercond. Nov. Magn. **29**, 569 (2016).
18. K. Yu. Arutyunov and J. S. Lehtinen, Nanoscale Res. Lett. **11**, 364 (2016).
19. K. Yu. Arutyunov and J. S. Lehtinen, Phys. C (Amsterdam, Neth.) **533**, 158 (2017).
20. K. Yu. Arutyunov, J. S. Lehtinen, A. A. Radkevich, A. G. Semenov, and A. D. Zaikin, J. Magn. Magn. Mater. **459**, 356 (2018).
21. K. Yu. Arutyunov, A. Ramos-Álvarez, A. V. Semenov, Yu. P. Korneeva, P. P. An, A. A. Korneev, A. Murphy, A. Bezryadin, and G. N. Gol'tsman, Nanotechnology **27**, 47LT021 (2016).
22. K. Yu. Arutyunov, S. V. Lotkhov, A. B. Pavolotski, D.A. Presnov, and L. Rinderer, Phys. Rev. B **59**, 6487 (1999).
23. K. Yu. Arutyunov, Phys. Rev. B **53**, 12304 (1996).
24. K. Yu. Arutyunov, T. V. Ryynanen, J. P. Pekola, and A. B. Pavolotski, Phys. Rev. B **63**, 092506 (2001).
25. V. V. Zavyalov, S. A. Chernyaev, K. V. Shein, A. G. Shukaleva, and K. Yu. Arutyunov, J. Phys.: Conf. Ser. **969**, 012086 (2018).
26. A. J. Annunziata, D. F. Santavicca, L. Frunzio, G. Catelani, M. J. Rooks, A. Frydman, and D. E. Prober, Nanotechnology **21**, 445202 (2010).
27. Z. M. Wang, J. S. Lehtinen, and K. Yu. Arutyunov, Appl. Phys. Lett. **114**, 242601 (2019).
28. G. Schön and A. D. Zaikin, Phys. Rep. **198**, 237 (1990).

Translated by G. Levina